Local interactions in carbon-carbon and carbon-M (M: Al, Mn, Ni) atomic pairs in FCC gamma -iron

1994 J. Phys.: Condens. Matter 6 679

(http://iopscience.iop.org/0953-8984/6/3/008)

J. Phys.: Condens. Matter 6 (1994) 679–692. Printed in the UK

Local interactions in carbon–carbon and carbon–M (M: Al, Mn, Ni) atomic pairs in FCC γ-iron

Katsuro Oda†, Hiroshi Fujimura and Hiromitsu Ino

Department of Materials Science, Faculty of Engineering, University of Tokyo, 7-3-1 Hongo Bunkyo-ku, Tokyo 113, Japan

Received 30 June 1993, in final form 19 October 1993

Abstract. Mössbauer spectra of Fe–8.0 at.%C, Fe–10.9 at.%Al–8.2 at.%C, Fe–1.4 at.%Mn–7.9 at.%C, Fe–2.4 at.%Mn–7.8 at.%C and Fe–14.6 at.%Ni–6.2 at.%C FCC γ-irons have been measured in order to investigate the distribution and the local interactions of C in the lattice. The local interaction energies in nearest and second-nearest C–C and M–C (M: Al, Mn, Ni) atomic pairs have been determined by a Monte Carlo method simulating the distribution obtained. The interaction energies in nearest and second-nearest C–C pairs are strongly repulsive, in contrast to the weak interaction in second-nearest N–N pairs. The results are compared with the interaction energies derived from activity data. The interaction in nearest Al–C pairs is repulsive but that in second-nearest pairs is strongly attractive, which can lead to the formation of the perovskite Fe_3AlC-type ordering. The interaction between nearest Mn and C atoms is strongly attractive, while between Ni and C the interaction is very weak.

1. Introduction

In FCC γ-iron, interstitial atoms such as carbon and nitrogen are known to occupy the octahedral interstitial sites in the FCC lattice. However, it has not yet been clarified how the atoms are distributed in the octahedral sites. Consequently, the local interaction energies between these atoms have not yet been determined. Up to now, the overall interaction energy between the interstitial atoms has been measured by means of thermodynamical measurements [1–4], from which, however, the local interaction energies such as those between the nearest-neighbouring (NN) or next-nearest-neighbouring (NNN) interstitial atoms cannot be derived.

Mössbauer spectroscopy is one of the most suitable methods for determining the local atomic structure around an Fe atom. Since 1967, a number of studies have been carried out to make clear the atomic structures of austenite (FCC Fe solid solute) for binary and ternary alloys [5–18]. However, no studies have derived the actual values of the local interaction energies from the Mössbauer spectrum. This is probably due to the lack of quantitativeness in the intensity ratio of the component spectra because of the thickness effect. As the thickness of the specimen increases, the absorption intensity has a tendency to deviate from a linear relation. In order to avoid this thickness effect, the present authors developed a new analysis method, which was applied to calculate the true component ratio of the Mössbauer spectrum for Fe–N austenite [18].

† Presently at Department of Materials Science, University of Tsukuba, 1-1-1 Tennoh-dai Tsukuba-shi, Ibaraki 305, Japan.

0953-8984/94/030679+14$07.50

In this paper, we apply this method to calculate the true component ratios for Fe–C and Fe–M–C (M: Al, Mn, Ni) γ-irons. Then we determine the values of the local interaction energies between C atoms, together with those between N atoms from the previously reported data [18], by the aid of a Monte Carlo simulation method. Furthermore, we estimate interaction energies between nearest and second-nearest Al–C, Mn–C and Ni–C pairs in the ternary alloys.

2. Experimental procedures

The Fe–C and Fe–M–C (M: Al, Mn, Ni) γ-iron specimens were prepared by electropolishing the ribbons melt-spun on a rotating copper wheel in an He atmosphere. From the x-ray diffraction measurements, Fe–Ni–C was shown to be a single γ-phase, while in Fe–C, Fe–Al–C and Fe–Mn–C a trace of BCT martensite phase (less than 1%) was found to exist. The compositions of the specimens were checked by chemical analysis to be Fe–8.0 at.%C, Fe–10.9 at.%Al–8.2 at.%C, Fe–1.4 at.% Mn–7.9 at.%C (Mn1), Fe–2.4 at.%Mn–7.8 at.%C (Mn2) and Fe–14.6 at.%Ni–6.2 at.%C.

The Mössbauer spectra were measured at room temperature using a 1 GBq ^{57}Co source. The velocity was calibrated by an α-iron reference. In order to correct the thickness effect and to determine the true fraction of the spectrum component, a number of spectra were measured for the same specimen with different thicknesses. The thickness of the absorber was controlled by changing the number of the stacked ribbons. From the thickness dependence of the apparent intensities of the component spectra, the true component ratios were determined by a method described elsewhere [18].

3. Results and discussion

3.1. Identification of the components

Figure 1 shows examples of Mössbauer spectra of Fe–C and Fe–M–C (M: Al, Mn, Ni) measured at room temperature. The spectra for Fe–C, Fe–Mn–C and Fe–Ni–C were decomposed into one single peak (γ_0) and a pair of peaks (γ_1), while in the spectrum for Fe–Al–C, another pair of peaks (γ_2) was found as shown in figure 1. The fitted parameters for the spectra are listed in table 1 together with those for Fe–N [18]. The values of isomer shift (IS) and quadrupole splitting (QS) of the decomposed spectra for Fe–C and Fe–Mn–C agree well with those of previous reports [5–15, 17]. For Fe–Al–C and Fe–Ni–C, the line width of the γ_0 component was broad and the fitting by a single peak was not satisfactory. Instead, we fitted the spectra by using a pair of peaks with quadrupole splitting of 0.14 mm s^{-1} for Fe–Al–C, and a six-line spectrum with a hyperfine splitting of 0.6 T for Fe–Ni–C.

The thickness dependences of the intensities of the spectral components for Fe–C and Fe–Al–C are shown in figure 2. The obtained true component ratios for each alloy are also listed in table 1.

The three components of the measured spectra can be assigned as follows [13, 14, 17, 18]:

γ_0: Fe atoms with no interstitial atoms at the NN sites (Fe(0))

γ_1: Fe atoms with one atom a the nearest sites (Fe(1)) or Fe atoms with two atoms placed at the two adjacent neighbouring sites (Fe(2, 90°))

γ_2: Fe atoms with two atoms placed at the opposite nearest sites (Fe(2, 180°)).

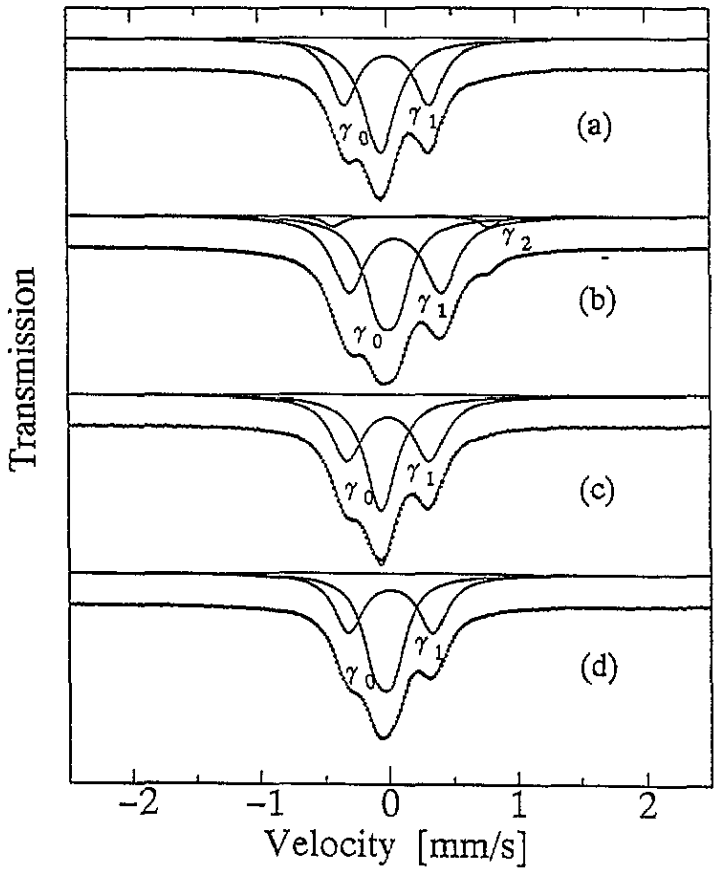

Figure 1. Mössbauer spectra of (*a*) Fe–8.0 at.%C, (*b*) Fe–10.9 at.%Al–8.2 at.%C, (*c*) Fe–2.4 at.%Mn–7.8 at.%C and (*d*) Fe–14.6 at.%Ni–6.2 at.%C together with the decomposed spectra.

The assignments of the γ_1 component to Fe(1) and/or Fe(2, 90°), and the γ_2 component to Fe(2, 180°) have been made under the assumption of the point charge approximation, so the electric field gradient can be superimposed [13, 14, 17, 18]. However, the value of QS for the γ_2 component of Fe–Al–C was not precisely twice that for γ_1, which indicates that the point charge approximation is not exact in this case.

These assignments imply that Fe(0), Fe(1) and/or Fe(2, 90°) and Fe(2, 180°) exist in Fe–Al–C γ-iron. On the other hand, in Fe–C, Fe–Mn–C and Fe–Ni–C, the Fe(2, 180°) structure does not exist, or even if it does, the proportion is less than the detectable limit of the present work (~ 0.5%). These results indicate that the interaction energy between the NNN C atoms is repulsive in Fe–C, Fe–Mn–C and Fe–Ni–C, while this is not the case for Fe–Al–C.

The group of Genin have measured the conversion electron Mössbauer spectra of Fe–C austenite, and obtained similar parameters for the γ_1 component to ours. They further decomposed the γ_0 component to those with and without NNN C atoms [17]. The γ_0 component of our spectra could not be separated so well.

The group of Bugayev has also observed the small hyperfine field at the Fe(0) site of the Fe–Ni–C alloy, which is due to the magnetic ordering [13]. The small quadrupole splitting observed at the Fe(0) site of Fe–Al–C is presumed to be due to the distortion that occurs

Table 1. The fitted isomer shift (IS), quadrupole splitting (QS) and the true component ratios of γ_0, γ_1 and γ_2 for each Mössbauer spectrum.

	γ_0		γ_1			γ_2		
Specimen	IS (mm s^{-1})	%	IS (mm s^{-1})	QS (mm s^{-1})	%	IS (mm s^{-1})	QS (mm s^{-1})	%
Fe–8.0 at.%C	−0.05	54.5	0.00	0.67	45.5	—	—	<0.6
Fe–10.9 at.%Al–8.2 at.%C	0.000 (QS ≈ 0.14)	60.0	0.06	0.72	36.5	0.19	1.20	3.0
Fe–1.4 at%Mn–7.9 at.%C	−0.05	64.0	0.00	0.67	36.0	—	—	<0.8
Fe–2.4 at.%Mn–7.8 at.%C	−0.06	64.0	0.00	0.66	36.0	—	—	<0.8
Fe–14.6 at.%Ni–6.2 at.%C	−0.03 (H_f ≈ 0.6 T)	67.0	0.02	0.57	33.0	—	—	<0.8
Fe–9.0 at.%N	0.01	47.3	0.08	0.39	49.6	0.20	0.72	3.0

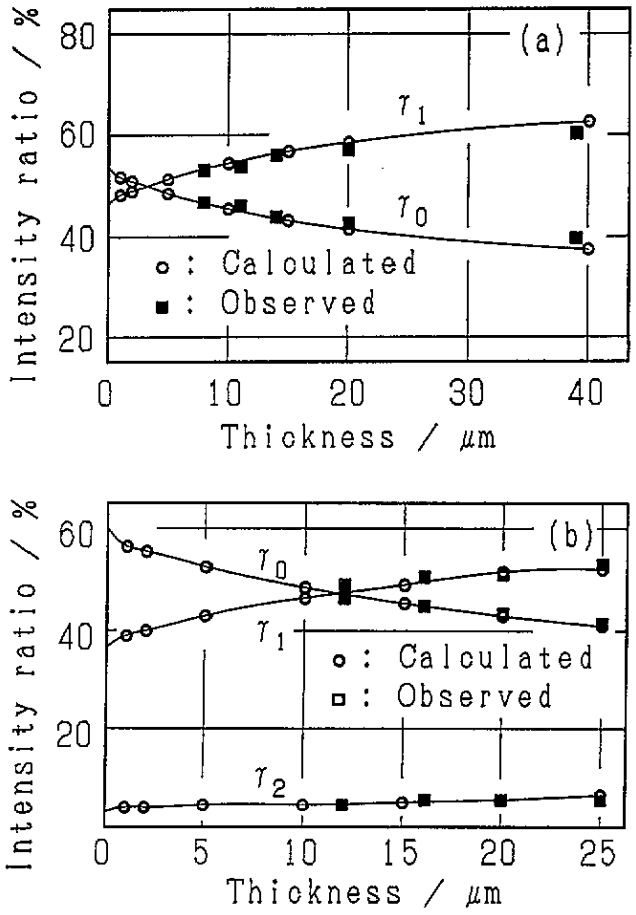

Figure 2. Thickness dependence of the intensities of the spectral components for (*a*) Fe–8.0 at.%C, (*b*) Fe–10.9 at.%Al–8.2 at.% C.

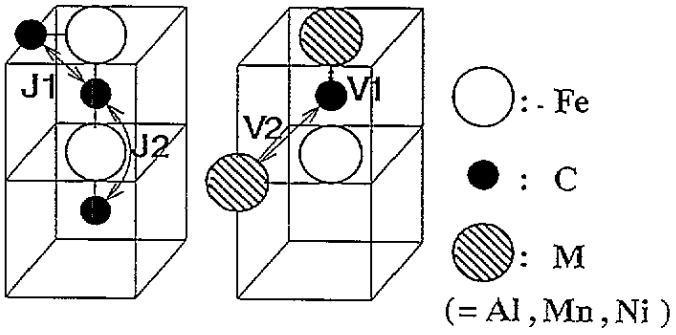

Figure 3. Definition of the interaction energies J_1 and J_2 between the NN and NNN C atoms, and the energies V_1 and V_2 between the NN and NNN M and C atoms.

by the occupation of Al atoms at the nearby sites.

3.2. Determination of the local interaction energies by Monte Carlo simulation

The ratio of local atomic configurations (Fe(0), Fe(1) and/or Fe(2, 90°), Fe(2, 180°)) corresponds to the true component fractions for γ_0, γ_1 and γ_2 ($I_{\gamma 0}$, $I_{\gamma 1}$ and $I_{\gamma 2}$), respectively, as mentioned in the previous section. On the other hand, the ratio of local atomic configurations is considered to be determined by the local atomic interaction energies J_1 and J_2 between the NN and NNN interstitial atoms, respectively (figure 3). However, it is not possible to calculate analytically the values of the interaction energies from the ratio of atomic configurations except for the case of dilute alloys [18]. In a strict sense, the interaction energies between further interstitial atoms (third nearest, fourth nearest and so on) should be taken into account; however, the magnitudes of these energies are considered to be smaller than J_1 and J_2. Therefore, in the present work, only the parameters of J_1 and J_2 are considered.

When assuming a dilute solution approximation, the ratio of local atomic configurations indicated by $I_{\mathrm{Fe}(0)}$, $I_{\mathrm{Fe}(1)}$, $I_{\mathrm{Fe}(2,90^\circ)}$ and $I_{\mathrm{Fe}(2,180^\circ)}$ can be expressed by

$$I_{\mathrm{Fe}(2,90^\circ)} = 12p^2 \exp(J_1/k_\mathrm{B}T) \qquad I_{\mathrm{Fe}(2,180^\circ)} = 3p^2 \exp(J_2/k_\mathrm{B}T)$$

$$I_{\mathrm{Fe}(1)} = 6p - 2I_{\mathrm{Fe}(2,90^\circ)} - 2I_{\mathrm{Fe}(2,180^\circ)} \qquad I_{\mathrm{Fe}(0)} = 1 - I_{\mathrm{Fe}(1)} - I_{\mathrm{Fe}(2,90^\circ)} - I_{\mathrm{Fe}(2,180^\circ)}.$$

J_1 and J_2 are defined to be positive when the interaction is attractive and vice versa [18] and p is the probability of the interstitial site occupancy. T and k_B are the temperature of the system and the Boltzmann constant, respectively.

Under this dilute alloy approximation, the local configurations are assumed to exist independently and no connected structures are considered. When the concentration of the interstitial atom is high, this approximation is inaccurate. Furthermore, for tenary alloys such as Fe–Al–C or Fe–Ni–C in which the third elements substitute the Fe sites, the effect of interaction between C and the substitutional atoms should be taken into account. Therefore, we adopted a numerical Monte Carlo simulation method to derive the atomic interaction energies. The procedure of the simulation is described below.

3.2.1. Monte Carlo simulation for Fe–C and Fe–N binary systems.

(a) Interstitial atoms are randomly distributed on the FCC lattice with a finite size of $30 \times 30 \times 30$ lattice points. It should be noted that the octahedral interstitial sites in the FCC lattice also construct an FCC lattice. The number of atoms is identical to the concentration of the alloy.

(b) Appropriate values of J_1 and J_2 are assumed. An atom is randomly chosen to make a jump to an arbitrary chosen NN site. The potential energy for the atom is given by

$$E_i = -(n_{i1}J_1 + n_{i2}J_2)$$

where n_{i1} and n_{i2} are the numbers of the NN and NNN atoms of the chosen atom, respectively.

(c) If the chosen site is already occupied by another atom, the jump is forbidden. If the change ΔE_i of energy is negative, the jump is allowed, and if positive, it is allowed with the probability of

$$p = \exp(-\Delta E_i/k_\mathrm{B}T).$$

(d) Steps (b) and (c) are repeated as many times as there are interstitial atoms and then the sum of the interaction energy E_i is calculated. This value is considered as the potential energy of the system E_{tot} after unit time.

(e) Steps (b)–(d) are repeated until the value of E_{tot} converges.

(f) The numbers of Fe(0), Fe(1), Fe(2, 90°) and Fe(2, 180°) in the system are counted and the component ratios of the configurations are obtained.

(g) If the calculated ratios coincide with the experimental ones obtained by the Mössbauer analysis, then the assumed values of J_1 and J_2 are considered to be correct. If they do not, the values are changed and steps (a)–(f) are repeated until the calculated ratios agree well with the experimental ones.

The best fit values of J_1 and J_2 for C atoms and N atoms are listed in table 2 together with those obtained assuming the dilute approximation. The values for N atoms are simulated by using the component ratios obtained in the previous report [18].

Table 2. The interaction energies between NN and NNN C and C or N and N atoms (J_1 and J_2) determined by Monte Carlo simulations together with those calculated assuming the dilute solution approximation; a positive value stands for attractive interaction and a negative value for repulsive interaction.

		Monte Carlo simulation	Dilute approximation
C–C	J_1/k_BT	-0.7 ± 0.2	-0.56
	J_2/k_BT	<-1.4	<-1.33
N–N	J_1/k_BT	-1.65 ± 0.15	-1.20
	J_2/k_BT	-0.20 ± 0.05	0.05

The values obtained from the Monte Carlo simulations are more repulsive than those obtained by assuming the dilute approximation. An example of the (001) plane of the simulated atomic configuration for Fe–C is shown in figure 4. Connection of Fe(2, 90°) structures can be seen in places. These connected structures are not taken into account in the dilute approximation, which is the reason why the values derived by dilute approximation are less repulsive.

3.2.2. Monte Carlo simulation or Fe–M–C (M: Al, Mn, Ni) ternary systems. For the Fe–M–C ternary systems, the interaction energies V_1 and V_2 (figure 3) between C and the NN and NNN M atoms are taken into account, together with J_1 and J_2. The following points are added to the procedure for the binary system.

(a′) The FCC lattice for Fe and M atoms with the same size of interstitial lattice is considered, and Fe and M atoms are randomly distributed on this new lattice.

(b′) The change in potential energy for the randomly chosen C atom is given by

$$E_i = -(n_{i1}J_1 + n_{i2}J_2 + m_{i1}V_1 + m_{i2}V_2)$$

where m_{i1} and m_{i2} are the number of NN and NNN M–C pairs.

(g′) The values of V_1 and V_2 are changed until the ratios of Fe(0), Fe(1), Fe(2, 90°) and Fe(2, 180°) obtained coincide with the experimental values. For J_1 and J_2, the fixed values obtained for the Fe–C binary system ($J_1 = -0.7k_BT$, $J_2 = -1.5k_BT$) are used.

The range of values of V_1 and V_2 derived from the simulations for Fe–Al–C, Fe–Mn–C and Fe–Ni–C is shown in figure 5. It should be noted that the interaction between NNN C and Al is attractive, while the NN interaction is repulsive. One of the simulated (001) planes for Fe–Al–C is shown in figure 6. Many Fe(2, 180°) structures are seen at the Fe sites where neighbouring Al atoms exist, compared with the sites surrounded by Fe atoms

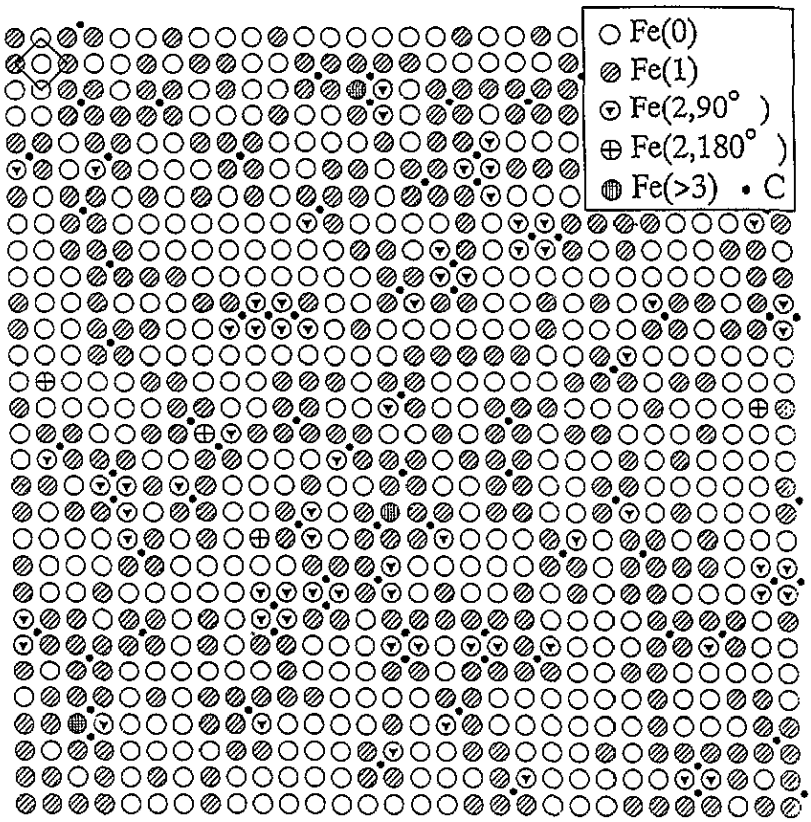

Figure 4. A (001) plane in Fe–8.0 at.%C simulated by the Monte Carlo method.

only. It can be concluded that an Al atom attracts two C atoms to assemble the Fe(2, 180°) structure. The attractive force would lead to the formation of the Fe_3AlC-type short-range order at temperatures when Al atoms can move for long distances.

The attractive interaction between the NN Mn–C pair is very strong ($\sim 6k_BT$). In the cases of Ni and C, the value is less than k_BT. However, the regions may expand to negative directions of V_2. This is because the γ_2 component is not observed for Fe–Mn–C and Fe–Ni–C, and only the upper limit of the value V_2 that corresponds to the detectable limit of the measurement can be determined.

3.3. Derivation of frozen temperature

In the previous section, the values of local interaction energies have been expressed in units of k_BT. To obtain the absolute values of local interaction energies (J_1, J_2, V_1 and V_2), the value of T should be estimated. This value is considered to be the temperature when the distribution of the interstitial atoms in the system is frozen during the cooling process of the specimen. First, when the melt is ejected on a copper roll, the specimen will be cooled at a rate of approximately 10^6–10^7 K s^{-1}. In the case of the melt quenching method, there exists little temperature gradient in the ribbon specimen of 20 μm thickness; therefore, the cooling rate is considered to be constant for the whole sample. Then, the specimen departs from the roll surface. From this instant, the specimen is cooled by the heat conductance of the He atmosphere and the cooling rate decreases drastically. The temperature of the

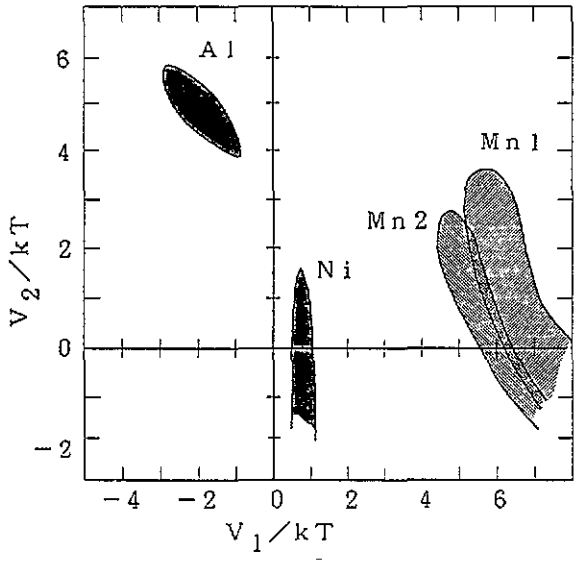

Figure 5. A map of interaction energies V_1 and V_2 between the NN and NNN M–C pairs (M: Al, Mn, Ni); a positive value stands for attractive interaction and a negative value for repulsive interaction.

specimen when it departs from the roll is certainly higher than 800 K by the observation of the colour of the specimen. Therefore, the diffusion of C atoms is not yet frozen at this time, and the cooling rate in the He atmosphere determines the freezing temperature.

Considering the heat conduction from the approximately 20 μm thick specimen to 1 atm He gas, the cooling rate is estimated to be about 10^3 K s^{-1}. Using this value, the frozen temperature of diffusion of the C atoms is estimated. The time τ necessary for a C atom to diffuse through a distance L is given by

$$\tau = L^2/D = L^2/[D_0 \exp(-Q/RT)]$$

where D is the diffusion constant of C in γ-iron, D_0 and Q are the frequency factor and the activation energy of diffusion, respectively, and R is the gas constant. During the cooling process, the diffusion rate of C atoms decreases, and there exists a frozen temperature T_f when the total diffusion length becomes less than one lattice constant of FCC γ-iron while the specimen is cooled to room temperature T_N. T_f can be given by

$$\frac{1}{a^2}\int_{T_N}^{T_f} D(T)\,dT = 1$$

where a is the lattice constant. The temperature T of the specimen is a function of time. T_f is estimated to be approximately 600 K. Then, the values of J_1 and J_2 are obtained as $J_1 = -3.5 \pm 1.0$ kJ mol^{-1} and $J_2 < -7.2$ kJ mol^{-1} for C atoms. For N atoms, the values are $J_1 = -8.2 \pm 0.7$ kJ mol^{-1} and $J_2 = -1.0 \pm 0.2$ kJ mol^{-1}.

3.4. Comparison with thermodynamically derived data

3.4.1. Fe–C and Fe–N binary systems. In the previous section, we estimated the absolute values of local interaction energies between C atoms or N atoms in FCC γ-iron. In this

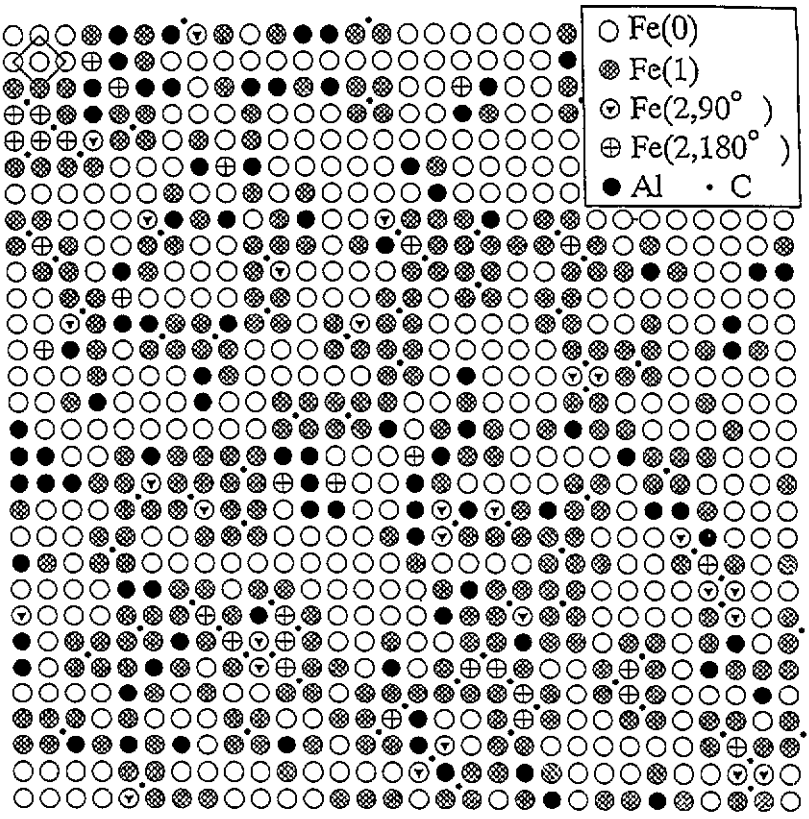

Figure 6. A (001) plane in Fe–10.9 at.%Al–8.2 at.%C simulated by a Monte Carlo method.

section, we compare them with the values calculated from the classical thermodynamical data by assuming a regular solution approximation [19] or applying a quasi-chemical method [4, 20, 21].

Based on a regular solution approximation, the enthalpy term of free energy for the Fe–C system can be described by the interaction energy ϵ_C between C atoms as

$$H = N(\chi_{Fe} z_{Fe} \epsilon_{Fe}/2 + \chi_C z_{FeC} \epsilon_{FeC} + \chi_C^2 z_C \epsilon_C / 2\chi_{Fe}) = (1-\chi_C) H_{Fe} + \chi_C \chi_{Fec} + [\chi_C^2/(1-\chi_C)]\chi_C.$$

Here

$$\chi_{Fe} = N z_{Fe} \epsilon_{Fe}/2 \qquad \chi_{FeC} = N z_{FeC} \epsilon_{FeC} \qquad \chi_C = N z_C \epsilon_C/2$$

where Z_{Fe} (= 12) and Z_{FeC} (= 6) are the coordination numbers of Fe atoms and C atoms, respectively, around an Fe atom. z_C (= 12) is that of C around a C atom. ϵ_{Fe} and ϵ_{FeC} are the interaction energies in Fe–Fe and Fe–C pairs, respectively. The activity of C can be written as

$$a_C = \chi_C \exp[(\chi_{FeC} - G_C^*)/RT] \exp[2(\chi_C + RT)/RT].$$

Here, the free energy of graphite at T K is taken as a standard.

Using the activity data measured for Fe–C γ-iron by Ban-ya and co-workers [22, 23] and assuming the regular solution approximation, Nishizawa showed that the value of interaction energy is

$$\epsilon_C = -0.07 \text{ eV/atom} = -6.8 \text{ kJ mol}^{-1}$$

at 1273 K [19]. Applying the same method to the data obtained by Atkinson and Bodsworth [24], the present authors calculated the interaction energy between N atoms to be

$$\epsilon_N = -3.4 \text{ kJ mol}^{-1}.$$

It should be noted that the several thermodynamical data for Fe–N are not consistent with each other [25] and there remains ambiguity in the value of ϵ_N.

Moreover, there exists a contradiction in this regular solution approximation: the solute atoms are assumed to be distributed randomly among the FCC interstitial sites. As can be seen from the present work, C or N atoms occupy the sites non-randomly. As a result of this, an apparent temperature dependence of ϵ_C will appear for the following reason. The number of C–C pairs used for calculating the enthalpy term $(Nz_C x_C^2/2(1 - x_C))$ is given by assuming a random distribution. When a repulsive interaction exists between C atoms, the number of pairs in the system should be less than the value derived assuming random distribution. As the temperature rises and the randomness increases, the former number of pairs approaches the latter value, and this leads to the temperature dependence of ϵ_C.

The quasi-chemical method is an improved approximation in that it takes into account the correlation of the atoms, and the distribution of atoms is not random in this treatment. The group of McLellan [4, 20] applied this method to the data measured by Ban-ya *et al* and by Atkinson and Bodsworth. They obtained $\epsilon_C = -8.0$ kJ mol^{-1} and $\epsilon_N = -4.0$ kJ mol^{-1}, which are stronger than the values obtained by assuming the regular solution approximation. Meanwhile, Lim *et al* [21] recently obtained $\epsilon_C = -6.86$ kJ mol^{-1} by a quasi-chemical method based on the data of Ban-ya *et al* , which is comparable to that obtained assuming the regular solution.

Table 3. Comparison between the overall interaction energy between C and C or N and N atoms $((z_1 J_1 + z_2 J_2)/2)$ determined by the present work, and $z_1\epsilon/2$ obtained by the regular solution [19] and quasi-chemical methods [4, 20, 21] based on thermodynamical measurements [22–24]. Values given are in kJ mol^{-1}.

	Present work			Regular solution	Quasi-chemical methods
	$z_1 J_1/2$	$z_2 J_2/2$	$(z_1 J_1 + z_2 J_2)/2$	$z_1\epsilon/2$	$z_1\epsilon/2$
C–C	−21	<−22	<−43	−41	~ −48–−41
N–N	−49	−3	−52	−20	− 24

From the present study, we have shown that J_2 is more repulsive than J_1 for C atoms in the γ-iron phase, while for N in γ-iron, J_1 is strongly repulsive and J_2 is weak. These results indicate that ϵ_C is determined by both J_1 and J_2, whereas J_1 dominates in ϵ_N. The total interaction energy in the system $z_1\epsilon/2$ can be roughly approximated as

$$z_1\epsilon/2 = (z_1 J_1 + z_2 J_2)/2.$$

The estimated values are < -43 kJ mol^{-1} for Fe–C and -52 kJ mol^{-1} for Fe–N (table 3). It is remarkable that the two values are almost the same. The value of the interaction energy

Table 4. The interaction energies between NN and NNN C and M (M: Al, Mn, Ni) atoms (V_1 and V_2) determined by Monte Carlo simulations, together with the interaction energy parameter W_{MC} derived from activity data; a positive value stands for an attractive interaction and a negative value for a repulsive interaction.

M	V_1 (kJ mol^{-1})	V_2 (kJ mol^{-1})	W_{MC} (kJ mol^{-1})
Al	−10	25	attractive
Mn	>26	<13	30 (at 1000 K)
Ni	~3.7–4.0	< 8	−30 (at 1000 K)

obtained by the present work agrees well with that obtained thermodynamically for the case of C atoms, but does not for N atoms. The adequacy of the present result is considered to be supported by the result of the change in lattice parameter.

The dependences of the lattice constant of FCC γ-iron on X_C and X_N, the concentrations of C and N, are reported as [26, 27]

$$a = 0.3572 + 0.078X_C \text{ (nm)}$$

and

$$a = 0.3560 + 0.084X_N \text{ (nm)}.$$

Recently, Cheng *et al* have modified the parameters as [28]

$$a = 0.3573 + 0.075X_C \text{ (nm)}$$

and

$$a = 0.3573 + 0.080X_N \text{ (nm)}.$$

The concentration dependences are very similar to each other. Moreover, we can find in the original data that as the concentration of C or N increases, the lattice constant deviates upwards from the linear relation. This tendency is common for C and N. The deviation is considered to originate from the repulsive interaction between interstitial atoms.

Cheng *et al* have discussed the fact that the covalent radius of C is larger than that of N [28], and Ishida *et al* have showed from the band structure calculations that the potential around N atoms is deeper than that for C atoms [29]. We have also reported in our previous paper that the electric field gradients of Fe(1) for Fe–C and Fe–N austenites are very different from each other [30]. The difference in the electronic structures affects the local interaction between Fe and the interstitial atoms. This may be the origin of the *different values of J_1 and J_2 for C and N.*

3.4.2. Interaction energies between C and M atoms (M: Al, Mn, Ni) in Fe–M–C ternary systems. The local interaction energies between C and M atoms (M: Al, Mn, Ni) in the Fe–M–C γ phase are listed in table 4, together with the interaction parameters W_{MC} derived from the activity data in thermodynamical measurements [31, 32]. Here, the value of T is taken to be 600 K as for the case of Fe–C. The attractive W_{AlC} is considered to originate from the strong attractive V_2 even though V_1 is repulsive, while both V_1 and V_2 could be effective for an attractive W_{MnC}. On the other hand, W_{NiC} is repulsive. In this case, the V_2 value was not determined by the present study for the reason previously mentioned, suggesting that V_2 is possibly repulsive.

It is known from the thermodynamical measurements that the solubility limit of C increases when alloying Al or Mn to the Fe–C γ phase, and decreases when alloying Ni [31,32]. It can be suggested that the increase in solubility is caused by the strongly attractive V_2 for Fe–Al–C and V_1 for Fe–Mn–C.

Since V_1 is repulsive and V_2 attractive in Fe–Al–C, it is presumed that Al atoms attract C atoms to the opposite two interstitial sites of the neighbouring Fe atom. The interactions are favourable for Fe_3AlC-type ordering. This leads to the formation of the perovskite Fe_3AlC (κ) phase when Al atoms can diffuse. On the other hand, it is possible that the attractive V_1 and V_2 cause the formation of carbides such as $(Fe,Mn)_3C$ or $(Fe,Mn)_{23}C_6$ in γ-Fe–Mn–C.

4. Conclusions

The distribution and local atomic configuration of C or N atoms in the Fe–C, Fe–N and Fe–M–C (M: Al, Mn, Ni) FCC γ phase have been determined by Mössbauer spectroscopy. By simulating the distribution by a Monte Carlo method, the local interaction energies in C–C, N–N and M–C atomic pairs have been determined. The interaction energies in NN and NNN C–C pairs are $J_1 = -3.5 \pm 1.0$ kJ mol^{-1} and $J_2 < -7.2$ kJ mol^{-1}, while for N–N pairs, the values are $J_1 = -8.2 \pm 0.7$ kJ mol^{-1} and $J_2 = -1.0 \pm 0.2$ kJ mol^{-1}.

The overall interaction energies between C atoms and N atoms calculated from these values are -6.8 kJ mol^{-1} and -3.4 kJ mol^{-1}, respectively.

For the interaction in Al–C pairs, the values were $V_1 = -10$ kJ mol^{-1} and $V_2 = 25$ kJ mol^{-1}. The repulsive V_1 and attractive V_2 for Al–C pairs is presumed to be the origin of the formation of Fe_3AlC-type ordered structure. The interaction between Mn and C is strongly attractive ($V_1 > 26$ kJ mol^{-1}), while between Ni and C, the interaction is very weak ($V_2 < 13$ kJ mol^{-1}).

Acknowledgments

The authors would like to express their sincere thanks to Professor Nobuo Sano of the Department of Metallurgy and Professor Kunio Ito of the Department of Materials Science for fruitful discussions. They would also like to express their thanks to Dr Setsuo Kajiwara of the National Research Institute of Metals for discussion and supplying the mother alloy of the specimens. The authors thank Mr Nobusato Kojima (presently with Sumitomo Metal Industries, Ltd) and Mr Kazuki Mae (presently a graduate student of the University of Tokyo) for their cooperation in the early stage of this work.

References

[1] Aaronson H I, Domain H A and Pound G M 1966 *AIME Trans.* **236** 753
[2] Alex K and McLellan R B 1971 *Acta Metall.* **19** 439
[3] Hillert M and Jarl M 1975 *Metall. Trans.* A **6** 553
[4] McLellan R B and Alex K 1970 *Scr. Metall.* **4** 967
[5] Gielen P M and Kaplow R 1967 *Acta Metall.* **15** 49
[6] Genin J M and Flinn A 1968 *Trans. Metall. Soc. AIME* **242** 1419
[7] Lesoille M and Gielen P M 1972 *Metall. Trans.* **3** 2681
[8] Gridynev V N, Gavrilyuk V G, Nemoshkalenko V N, Polushkin Yu A and Razumov O N 1977 *Fiz. Met. Metallov.* **43** 582

[9] DeCristofaro N and Kaplow R 1977 *Metall. Trans* A **8** 35
[10] Litvinov V S, Karakishev S D and Tsurin V A 1977 *Fiz. Met. Metallov.* **43** 108
[11] Williamson D L, Nakazawa K and Krauss G 1979 *Metall. Trans.* A **10** 1351
[12] Kozlova O S and Makarov V A 1979 *Fiz. Met. Metallov.* **48** 63
[13] Bugayev V N, Gavrilyuk V G, Nadutov V N and Tatarenko V A 1983 *Acta Metall.* **31** 407
[14] Ino H, Umezu K, Kajiwara S and Uehara S 1986 *Proc. Int. Conf. on Martensitic Transformations* (Sendai: Japan Institute of Metals) p 313
[15] Bugayev V N, Gavrilyuk V G, Nadutov V N and Tatarenko V A 1986 *Sov. Phys.–Dokl.* **31** 439
[16] Foct J, Rochegude P and Hendry A 1988 *Acta Metall.* **36** 501
[17] Uwakweh O N C, Bauer J Ph and Genin J M 1990 *Metall. Trans.* A **21** 589
[18] Oda K, Umezu K and Ino H 1990 *J. Phys.: Condens. Matter* **2** 10147
[19] Nishizawa T 1973 *Bull. Japan. Inst. Met.* **12** 321
[20] Dunn W W and McLellan R B 1970 *Metall. Trans.* **1** 1267
[21] Lim S H, March G E and Oates W A 1989 *CALPHAD* **13** 139
[22] Ban-ya S, Elliot J F and Chipman J 1969 *Trans. Metall. Soc. AIME* **245** 1199
[23] Ban-ya S, Elliot J F and Chipman J 1970 *Metall. Trans.* **1** 1313
[24] Atkinson D and Bodsworth C 1970 *J. Iron Steel Inst.* **208** 587
[25] Japan Society for the Promotion of Science 1988 *Steelmaking Data Sourcebook* (London: Gordon and Breach)
[26] Jack K H 1951 *Proc. R. Soc.* A **208** 427
[27] Ruhl R C and Cohen M 1969 *AIME Trans.* **245** 241
[28] Cheng L, Böttger A, de Keijser Th H and Mittemeijer E J 1990 *Scr. Met. Mater.* **24** 509
[29] Ishida S, Kitawatase K, Fujii S and Asano S 1992 *J. Phys.: Condens. Matter* **4** 765
[30] Oda K, Fujimura J, Mae K and Ino H 1991 *Hyperfine Interact.* **69** 533
[31] Hsin E and Lupis C H P 1973 *Acta Metall.* **21** 2409
[32] Nishizawa T 1973 *Bull. Japan. Inst. Met.* **12** 401